Longitudinal spin dynamics in the Heisenberg ferromagnet: Diagrammatic approach

Yu. A. Izyumov,[1,2] N. I. Chaschin,[2] and V. Yu. Yushankhai[1,3]
[1]*Max-Planck-Institut für Physik Komplexer Systeme, D-01187 Dresden, Germany*
[2]*Institute for Metal Physics, Ural Division of the Russian Academy of Science, 620219 Ekaterinburg, Russia*
[3]*Joint Institute for Nuclear Research, 141980 Dubna, Russia*
(Received 18 July 2001; revised manuscript received 14 January 2002; published 7 June 2002)

Based on the diagrammatic technique for spin operators, the ferromagnetic Heisenberg model is studied with an emphasis on the longitudinal spin dynamics. The diagram rules are, to our knowledge, newly formulated by using equations in terms of variational derivatives of a generating functional describing interactions of the spin system with auxiliary fluctuating fields. This approach provides us with an efficient procedure to derive graphical representations for perturbation expansion series for different spin Green functions. Since fluctuations of the longitudinal spin components are generated by processes of virtual creation and annihilation of transverse spin component modes (renormalized spin waves), the infinite series involving all distinct loops built from spin-wave propagators are summed up. This results in an expression for the longitudinal spin susceptibility $\chi^{zz}(\mathbf{q},\omega)$ taking a generalized RPA-type form with a strongly renormalized denominator including all the terms $\sim 1/z$ (z is the first coordination lattice number). The corresponding longitudinal component of the dynamic structure factor exhibits a three-peak structure with two wide maxima at frequencies $\Omega_q \sim \pm J\langle S^z\rangle q$ and a sufficiently narrow central peak that grows fast when approaching the Curie temperature. With growing temperature, the intensity of the Ω_q peaks increases, and they merge with the central peak whereas the width of the entire spectral distribution decreases. At fixed temperature, the distribution width changes linearly with wave vector q. The observed picture is applicable beyond the hydrodynamic regime that is valid at small q and higher temperatures. Study of the evolution of the spectral distribution from a three-peak structure to a single-peaked one, valid beyond the hydrodynamic regime, with increasing temperature can help to explain conflicting results of neutron studies of longitudinal fluctuations in different ferromagnets.

DOI: 10.1103/PhysRevB.65.214425 PACS number(s): 75.10.Jm, 75.10.−b, 78.70.Nx

I. INTRODUCTION

One of the basic models of the theory of magnetism is the Heisenberg lattice model with the Hamiltonian

$$H = -\frac{1}{2}\sum_{ij} J_{ij}(\mathbf{S}_i\mathbf{S}_j). \tag{1.1}$$

Here $\mathbf{S}_i$ is the spin operator on an ith lattice site, J_{ij} is the exchange integral. Despite its simple definition even in the case of ferromagnetic coupling, $J_{ij}>0$, the statistical mechanics of the model in a wide range of temperatures is far from being trivial. Within this context, several basic notions and theoretical approaches to the problem are worth mentioning. As it is well known,[1] the concept of spin waves as low-energy collective excitations describing the dynamics of transverse spin components provides a good approximation at low temperatures. Effects of spin-wave interactions were highlighted by Dyson.[2] Bogoliubov and Tyablikov gave rather a simple extrapolation theory[3] and extended the spin-wave concept to higher temperatures $T<T_C$ (T_C is the Curie temperature). They showed that the temperature-renormalized spin-wave energy spectrum is described by a standard expression for the spin-wave dispersion if the maximum spin projection S is replaced by its average value $\langle S^z\rangle$. However, the spin-wave decay processes were not considered in Ref. 3. Vaks, Larkin, and Pikin[4] (VLP) examined this problem and argued that in the long-wave limit, the decay rate of the renormalized spin waves remains to be comparatively small even in the high-temperature regime at $T<T_C$ and, hence, these elementary spin excitations survive up to the critical vicinity of T_C. These theoretical predictions were confirmed in many inelastic neutron scattering measurements of ferromagnetic materials (see, for instance, Ref. 5 and references therein).

Study of the dynamics of longitudinal spin components implies a different physical picture and poses new theoretical problems. Both the theoretical predictions and experimental results available in this area are rather scarce and contradictory.[6] According to VLP, a longitudinal spin mode arises as a result of a virtual process of coherent creation and annihilation of ordinary spin waves. By developing a regular perturbative approach and further using some simplifying approximations, VLP evaluated the spectral density of the longitudinal spin correlation function, i.e., the imaginary part of the longitudinal susceptibility $\chi^{zz}(\mathbf{q},\omega)$. The calculated $\chi^{zz}(\mathbf{q},\omega)$ has shown two weak resonances at frequencies $\omega = \pm\varepsilon(\mathbf{q})$, where $\varepsilon(\mathbf{q})$ is the energy of a spin wave at the same momentum $\mathbf{q}$. Consequently, the measurements of the longitudinal spin fluctuations at $T<T_C$ in inelastic neutron scattering experiments should reveal two symmetric resonance peaks.

At the same time it was predicted that at $T>T_C$, but beyond the critical region, the spectral density of spin fluctuations in the hydrodynamic regime where the transverse and longitudinal spin fluctuations are indistinguishable is described by the van Hove formula

$$\chi(\mathbf{q},\omega) \sim \frac{1}{\pi}\frac{\Lambda q^2}{\omega^2 + (\Lambda q^2)^2}. \tag{1.2}$$

Here Λ is proportional to the coefficient of spin diffusion. Motivated by this observation, VLP suggested that in an ordered state, $T<T_C$, the longitudinal dynamics of spin fluctuations at small $\mathbf{q}$ and ω acquires a diffusive feature to give a three-peaked structure of $\chi^{zz}(\mathbf{q},\omega)$: there are two inelastic peaks at $\omega=\pm\varepsilon(\mathbf{q})$ and a narrow quasielastic peak at $\omega=0$ of the width $\sim\Lambda q^2$. This suggestion was not confirmed, however, in subsequent theoretical studies. For instance, Villan[7] obtained a two-peak structure, whereas Mazenko[8] predicted a broad quasielastic peak in $\chi^{zz}(\mathbf{q},\omega)$.

Experimental investigations of the longitudinal spin fluctuations in ferromagnetic materials led to contradictory results as well. The studies carried out in pure iron[9] and nickel[10] close to but below T_C revealed an inelastic two-peaked structure of $\chi^{zz}(\mathbf{q},\omega)$ without any signature of the central peak. A two-peaked shape of $\chi^{zz}(\mathbf{q},\omega)$ similar to the spin-wave spectrum was found[11] also in nonmetallic ferromagnets EuO and EuS considered to be a prototype of the Heisenberg model. On the contrary, a quasielastic single-peak behavior without evidences of the resonant scattering was observed[6] by the neutron scattering technique in the ferromagnetic Pd-Fe alloy. In this experiment, a spin polarization analysis was performed to distinguish contributions from longitudinal and transverse spin fluctuations. A similar picture was observed also in the study[12] of the longitudinal spin dynamics in the antiferromagnetic $RuMnF_3$.

In view of the unsettled situation, both in the theory and experiment, new theoretical approaches to the problem of the longitudinal spin dynamics are strongly required. In the recent study by Bunker and Landau,[13] spin dynamics simulations with finite clusters were used to calculate the longitudinal component of the dynamic structure factor that, in fact, is the imaginary part of the longitudinal spin susceptibility $\chi^{zz}(\mathbf{q},\omega)$. Only the classical limit, $S\to\infty$, of the Heisenberg model at high temperatures was considered both for ferromagnetic (FM) and antiferromagnetic (AFM) cases. For the FM case, the excitation peaks are found at frequencies $\omega^-(\mathbf{q})=|\varepsilon(\mathbf{k})-\varepsilon(\mathbf{k}\pm\mathbf{q})|$ and interpreted in terms of processes of creation and annihilation of two spin waves with energies $\varepsilon(\mathbf{k})$ and $\varepsilon(\mathbf{k}\pm\mathbf{q})$. For the AFM case, there is also a second channel of two-spin-wave excitations with the energy $\omega^+(\mathbf{q})=|\varepsilon(\mathbf{k})+\varepsilon(\mathbf{k}\pm\mathbf{q})|$. In both expressions for $\omega^{\pm}(\mathbf{q})$, the wave vector $\mathbf{k}$ is a variable. The excitation processes are controlled, however, by the occupation factor [determined through the momentum Bose distribution function $n(\mathbf{k})$], which makes the spin waves with $\mathbf{k}\sim 0$ to be dominant ones. Therefore, the positions of excitation peaks measured by $\mathrm{Im}\,\chi^{zz}(\mathbf{q},\omega)$ are close to spin-wave energies $\varepsilon(\mathbf{q})$. Thus, the numerical study[13] of the classical limit of the Heisenberg model has confirmed the multiple spin-wave nature of the propagating longitudinal spin excitation in accordance with the basic idea elaborated in the quantum case by VLP in their pioneering work.[4] We note, however, that simplifying and uncontrolled approximations used in Ref. 4 impose strong restrictions on the validity of the expression for the longitudinal spin susceptibility derived there.

In the present paper, we study the longitudinal spin dynamics of the ferromagnetic quantum Heisenberg model. We develop a general theoretical treatment aiming to overcome some limitations contained in Ref. 4 and to reveal a unique physical picture common to numerous experimental observations mentioned above. Relying on the diagrammatic technique in terms of spin operators proposed and elaborated by VLP in the late sixties,[4] we use below a convenient version of this technique developed later by one of the present authors.[14–16] A detailed account of this version is given in the monograph[15] available to Russian readers, and a strongly compressed description is presented also in Ref. 16. Up to now, when the diagrammatic technique[4,14–16] was constructed the Wick theorem for the spin operators was used. In the present paper, we follow a new way and develop an approach based on a generating functional describing interactions of the spin system with auxiliary fluctuating fields. Spin Green functions (GFs) are determined as variational derivatives with respect to these fields. The procedure can be considered as a generalization of the famous Baym-Kadanoff approach[17] in the theory of usual Bose (Fermi) systems.

In Secs. II–IV, we show that the diagrammatic series for spin GFs arise as a result of the Taylor series expansion of a specially defined generating functional. As compared to the standard perturbative scheme based on the Wick theorem, the present approach gives more efficient and straightforward prescriptions to handle the spin GFs. Another advantage of the generating functional method is that it provides a way to easily derive exact equations in terms of functional derivatives for different spin GFs, which enables one to test different approximate solutions of these exact equations. A more detailed discussion comparing the generating functional method with the standard one is presented in Secs. II–IV.

In Sec. V, a diagrammatic representation for the longitudinal spin GF is formulated. Since the quantum dynamics of longitudinal spin components is generated by virtual processes of creation and annihilation of spin waves, the mathematical problem amounts to summing up all the loop diagrams describing these processes. A complexity of the problem arises from the fact that a commutator of two spin operators, for instance, S_i^+ and S_i^-, is not a c number. Therefore, the series of the loop diagrams turns out to be rather complicated and contains four different types of loops. To sum up these series, we use a method called GRPA (generalized random-phase approximation) elaborated earlier by one of the present authors[18,19] in the study of the t-J model formulated in terms of Hubbard X operators. When an appropriate diagrammatic technique is applied to the t-J model and collective Bose-type modes are calculated, also series are obtained for loop diagrams with four types of distinguishable loops. Though the loop diagrams for the Heisenberg model and the t-J model are defined in terms of bosonic spin-wave GFs and fermioniclike propagators, respectively, the diagrammatic series for both the models are very similar. The isomorphic character of diagrammatic series for these two different models originates from the fact that permutation relations between a pair of the Bose-like operators X^{+-} and X^{-+} within the t-J model is of the same structure as that for spin operators S^+ and S^- for the spin model. By summing up all the loop diagrams, we arrive, at the end of Sec. V, at the final expression for the longitudinal GF the denomi-

nator of which includes all the terms $\sim 1/z$ (z is the first coordination number of a relevant magnetic lattice).

Analytic continuation of the Matsubara-type spin GFs onto the real ω axis determines the longitudinal susceptibility $\chi^{zz}(\mathbf{q},\omega)$ of the Heisenberg model. In Secs. VI, VII, the susceptibility is examined as a function of frequency ω and wave vector $\mathbf{q}$. This analysis shows that fluctuational dynamics of longitudinal spin components corresponds to two strongly damped oscillators coexisting with a relatively narrow central peak or a broad diffusive peak in the relevant spectral distribution. Respectively, either a three-peaked or an entire single-peaked shape of the longitudinal component of the dynamic structure factor is expected, which is controlled by temperature and a relevant set of parameters of the magnetic system under consideration. We believe that this property of the calculated longitudinal spin susceptibility provides an explanation of the apparently conflicting results obtained in different inelastic neutron scattering measurements of ferromagnetic materials.

II. GENERATING FUNCTIONAL AND SPIN GREEN FUNCTIONS

We start with a more general anisotropic spin model by introducing the Hamiltonian

$$H=-h\sum_i S_i^z-\sum_{ij} S_i^+ J_{ij} S_j^- -\frac{1}{2}\sum_{ij} S_i^z J_{ij}^z S_j^z, \quad (2.1)$$

where the circular spin operators are defined as follows $S_i^{\pm}=(S_i^x \pm iS_i^y)/\sqrt{2}$. In the limit $J_{ij}^z=J_{ij}$ and at the zero external field, $h=0$, the isotropic Heisenberg model (1.1) is restored. This is supplemented by the commutation relations

$$[S_i^z,S_j^{\pm}]=\pm\delta_{ij}S_i^{\pm}, \quad [S_i^+,S_j^-]=\delta_{ij}S_i^z. \quad (2.2)$$

Let us now introduce a partition function $Z=\mathrm{Tr}(e^{-\beta H})$ with β being the inverse temperature, and define spin Green functions

$$K(i\tau,j\tau')=\langle TS_i^-(\tau)S_j^+(\tau')\rangle, \quad (2.3)$$

$$K^{zz}(i\tau,j\tau')=\langle TS_i^z(\tau)S_j^z(\tau')\rangle. \quad (2.4)$$

Here $S_i^{\alpha}(\tau)$ are components ($\alpha=x,y,z$) of the spin operator in the Heisenberg representation with imaginary time τ:

$$S_i^{\alpha}(\tau)=e^{H\tau}S_i^{\alpha}e^{-H\tau},$$

and the ''time'' varies in the region $0<\tau<\beta$. In Eqs. (2.3), (2.4), T is the time-ordering operator, and $\langle\cdots\rangle$ denotes the Gibbs ensemble averaging

$$\langle\cdots\rangle=\mathrm{Tr}(e^{-\beta H}\cdots)/\mathrm{Tr}\,e^{-\beta H}.$$

With the Hamiltonian (2.1), the equations of motion for spin operators can be straightforwardly written as

$$\dot{S}_i^-=-[S_i^-,H]=hS_i^- -S_i^z\sum_j J_{ij}S_j^- +S_i^-\sum_j J_{ij}S_j^z, \quad (2.5)$$

$$\dot{S}_i^z=-[S_i^z,H]=S_i^+\sum_j J_{ij}S_j^- -\sum_j S_j^+ J_{ji}S_i^-. \quad (2.6)$$

To calculate spin GFs, we first define a generating functional $Z[V]$ in the following form of a generalized partition function Z,

$$Z[V]=\mathrm{Tr}(e^{-\beta H}Te^V), \quad (2.7)$$

where the operator variable V contains fluctuating fields acting on the spin system. For our purposes, the following appropriate form of V is chosen:

$$V=v_{1'}S_{1'}^z+S_{1'}^+u_{1'2'}S_{2'}^-. \quad (2.8)$$

Here the numerical suffixes are composite ones, and each designates a lattice site and a time variable like, for instance, $1=(i_1,\tau_1)$. Each pair of repeating suffixes implies the summation over the sites and the time integration over the interval $0<\tau<\beta$. Hereafter such suffixes are primed.

The time-ordered products of spin operators can now be defined as variational derivatives of $Z[V]$. In particular, the derivatives

$$\frac{\delta Z}{\delta v_1}=\mathrm{Tr}(e^{-\beta H}TS_1^ze^V)\equiv Z[V]\langle TS_1^z\rangle_V,$$

$$\frac{\delta Z}{\delta u_{12}}=\mathrm{Tr}(e^{-\beta H}TS_1^-S_2^+e^V)\equiv Z[V]\langle TS_1^-S_2^+\rangle_V,$$

$$\frac{\delta^2 Z}{\delta v_1\delta v_2}=\mathrm{Tr}(e^{-\beta H}TS_1^zS_2^ze^V)\equiv Z[V]\langle TS_1^zS_2^z\rangle_V, \quad (2.9)$$

being taken at $v_1,u_{12}=0$, give the expectation value $\langle S_1^z\rangle$ and the spin GFs (2.3), (2.4). In Eq. (2.9) the notation $\langle\cdots\rangle_V$ means

$$\langle\cdots\rangle_V=\frac{\mathrm{Tr}(e^{-\beta H}\ldots e^V)}{\mathrm{Tr}(e^{-\beta H}e^V)}. \quad (2.10)$$

With the definition $Z=e^{\Phi}$ giving another functional Φ, an analog of the free energy, we rewrite the expressions (2.9) in the following form:

$$\frac{\delta\Phi}{\delta v_1}=\langle S_1^z\rangle_V,$$

$$\frac{\delta\Phi}{\delta u_{12}}=\langle TS_1^-S_2^+\rangle_V,$$

$$\frac{\delta^2\Phi}{\delta v_1\delta v_2}=\langle T(S_1^z-\langle S_1^z\rangle)(S_2^z-\langle S_2^z\rangle)\rangle\equiv\langle TS_1^zS_2^z\rangle_V^c. \quad (2.11)$$

In Eq. (2.11), the notation $\langle\cdots\rangle_V^c$ denotes a connected GF.

Evolution of spin GFs in fluctuating fields is obtained by using the equations of motion for spin operators. Let us first consider the transverse GF, $\langle TS_1^-S_2^+\rangle_V$. According to the

prescriptions presented in the Appendix (a new notation is introduced there as well), the evolution of this GF is governed by the equation

$$\frac{\partial}{\partial\tau_1}((TS_1^-S_2^+e^V))=((T[S_1^-,S_2^+]e^V))+((T\{S_1^-,V\}S_2^+e^V))$$
$$+((T\dot{S}_1^-S_2^+e^V)). \tag{2.12}$$

To bring Eq. (2.12) closer to our main notation we first present Eq. (2.5) for S_1^- in the form with composite numerical arguments,

$$\dot{S}_1^-=hS_1^--\alpha_0(11';3')S_{3'}^zS_{1'}^-, \tag{2.13}$$

where

$$\alpha_0(12;3)=\delta_{13}J_{12}-\delta_{12}J_{13}^z, \tag{2.14}$$

and $J_{12}=\delta(\tau_1-\tau_2)J_{i_1i_2}$. By using also the definition (see the Appendix)

$$\{S_1^-,V\}=v_1S_1^--S_1^zu_{11'}S_{1'}^-, \tag{2.15}$$

one obtains, from Eq. (2.12), the explicit equation for the transverse GF as follows:

$$-\left(\frac{\partial}{\partial\tau_1}-\tilde{v}_1\right)((TS_1^-S_2^+e^V))=\delta_{12}((TS_1^ze^V))+\tilde{\alpha}_0(11';3')$$
$$\times((TS_{1'}^-S_2^+S_{3'}^ze^V)). \tag{2.16}$$

Here $\tilde{v}_1=v_1+h_1$ and $\tilde{\alpha}_0$ is given by Eq. (2.14) after the replacement $J_{12}\to\tilde{J}_{12}=J_{12}+u_{12}$. Following the main line of the generating functional method, all the averages of T products can be expressed here through the corresponding variational derivatives either with respect to v_1 and u_{12} or, equally well, to h_1 and J_{12} due to the additivity of $\tilde{v}_1$ and $\tilde{J}_{12}$. From now on, h_1 and J_{12} are treated as some general fluctuating fields. Finally, the equation for the transverse GF reads

$$\left[k_{11'}^{(0)-1}-\left(\alpha_0\frac{\delta\Phi}{\delta h}\right)_{11'}-\left(\alpha_0\frac{\delta}{\delta h}\right)_{11'}\right]\frac{\delta\Phi}{\delta J_{1'2}}=\delta_{12}\frac{\delta\Phi}{\delta h_2}, \tag{2.17}$$

where

$$k_{11'}^{(0)-1}=-\left(\frac{\partial}{\partial\tau_1}-h_1\right)\delta_{11'}. \tag{2.18}$$

[Here and below we adopt a compact notation like, for instance, $(\alpha_0X)_{12}\equiv\alpha_0(12;3')X_{3'}$]. More generally, Eq. (2.17) should be considered as a differential equation for the generating functional $\Phi=\Phi[h,J,J^z]$ in arbitrary fluctuating fields h,J,J^z, and the relations (2.11) should be rewritten as

$$\frac{\delta\Phi}{\delta h_1}=\langle S_1^z\rangle_V, \tag{2.19}$$

$$\frac{\delta\Phi}{\delta J_{12}}=\langle TS_1^-S_2^+\rangle_V, \tag{2.20}$$

$$\frac{\delta^2\Phi}{\delta h_1\delta h_2}=\langle TS_1^zS_2^z\rangle_V^c. \tag{2.21}$$

Thus, with a given solution $\Phi[h,J,J^z]$, the actual GFs are found by taking derivatives of Φ at $J_{12}=\delta(\tau_1-\tau_2)J_{i_1,i_2}$.

A sequence of equations in terms of higher-order derivatives of Φ is generated by differentiating the main equation (2.17) with respect to h. Along this way, approximate solutions of Eq. (2.17) can be found. This procedure will be helpful at some stage of our derivation (Sec. IV). At the present stage, we are dealing directly with Eq. (2.17) by rewriting it first as follows:

$$\hat{k}_{11'}^{-1}\frac{\delta\Phi}{\delta J_{1'2}}=\delta_{12}\frac{\delta\Phi}{\delta h_2}, \tag{2.22}$$

where the differential operator

$$\hat{k}_{11'}^{-1}\equiv k_{11'}^{(0)-1}-\left(\alpha_0\frac{\delta\Phi}{\delta h}\right)_{11'}-\left(\alpha_0\frac{\delta}{\delta h}\right)_{11'} \tag{2.23}$$

is introduced. We are looking for a solution of Eq. (2.22) in the following factorized form:

$$\frac{\delta\Phi}{\delta J_{12}}=k_{11'}P_{1'2}. \tag{2.24}$$

By inserting Eq. (2.24) into the original Eq. (2.22), one arrives at a couple of equations for k_{12} and P_{12}:

$$k_{12}^{-1}=k_{12}^{(0)-1}-\left(\alpha_0\frac{\delta\Phi}{\delta h}\right)_{12}+k_{4'3'}\left(\alpha_0\frac{\delta}{\delta h}\right)_{14'}k_{3'2}^{-1}, \tag{2.25}$$

$$P_{12}=\delta_{12}\frac{\delta\Phi}{\delta h_2}+k_{4'3'}\left(\alpha_0\frac{\delta}{\delta h}\right)_{14'}P_{3'2}. \tag{2.26}$$

By applying an iteration procedure, we derive below the series for the quantity P_{12} that we call the terminal part, and for k_{12} that should be referred to as the Dyson propagator. The latter is reasoned by the fact that the quantity $k_{12}^{(0)}$ entering into Eq. (2.25) is the propagator of the transverse GF for the noninteracting case. If interaction is switched on, a self-energy part (a mass operator) is defined in a standard way,

$$k_{12}^{-1}=k_{12}^{(0)-1}-M_{12}. \tag{2.27}$$

Then it follows from Eq. (2.25) that M should satisfy the following equation:

$$M_{12}=\left(\alpha_0\frac{\delta\Phi}{\delta h}\right)_{12}-\alpha_0(11';2)k_{1'2}+k_{4'3'}\left(\alpha_0\frac{\delta}{\delta h}\right)_{14'}M_{3'2}. \tag{2.28}$$

As the next step of our derivation (Sec. III), we apply a properly defined iteration procedure and develop the mass operator M and the terminal part P of the transverse spin GF into perturbative series, which is equivalent to a regular diagrammatic expansion in terms of spin operators.[4,14] The it-

eration procedure appears to be rather complicated and is based on a successive differentiating of M, P, and k with respect to h.

III. SERIES EXPANSION OF GENERATING FUNCTIONAL AND DIAGRAMMATIC TECHNIQUE FOR SPIN GREEN FUNCTIONS

Equations (2.25) and (2.26) are the basic ones for developing a perturbation theory for spin GFs. This will be accomplished in a few steps.

(1) First, we obtain a formal series expansion of the transverse spin GF in powers of exchange parameters J and J^z. To this end, Eqs. (2.25) and (2.26) are treated iteratively, which gives certain intermediate formal expressions containing variational derivatives of Φ with respect to h of different orders.

(2) To calculate these derivatives, a Taylor series expansion of Φ with J and J^z varying in the neighborhood of $J=J^z=0$ is derived. The coefficients of this series taken at $J=J^z=0$ are found by differentiating Eq. (2.24) with respect to J and J^z sequentially.

(3) By differentiating the above Taylor series with respect to a field h and using Eqs. (2.19) and (2.21), one is able now to find perturbative expansions both for an average spin projection and the longitudinal GF. With a subsequent substitution of these expansions into the iterative terms of Eqs. (2.25) and (2.26) the corresponding perturbative expansion of the transverse GF is obtained as well.

Such a rather sophisticated procedure is inevitable when searching for a desirable perturbative series expansion for quantities defined in Eqs. (2.19)–(2.21) that are connected with each other in a nonlinear way. Below we apply this procedure to obtain the perturbative series for the above-mentioned quantities up to the second order in J. All the main ingredients of our perturbation theory arise already at this stage. Going further, we will show that there is a perfect correspondence between the series resulting from our approach and the one appearing in the standard diagrammatic technique based on the Wick theorem for spin operators. At the same time, the present approach provides a more fast-acting procedure allowing us to formulate the corresponding rules of the diagrammatic technique. Moreover, our approach handles variational derivatives and thus operates with ''exact'' GFs. Therefore, the coefficients of different perturbative series resulting from our analysis involve exact GFs. In the context of the standard diagrammatic technique, this means that some of the infinite series are already summed up.

After these preliminaries, we proceed to considering the following Taylor expansion of the generating functional with respect to fluctuating fields J and J^z:

$$\Phi[h,J,J^z]=\Phi_0[h]+J_{2'1'}\left(\frac{\delta\Phi}{\delta J_{1'2'}}\right)^0+J^z_{2'1'}\left(\frac{\delta\Phi}{\delta J^z_{1'2'}}\right)+\frac{1}{2!}\left[J_{2'1'}J_{4'3'}\left(\frac{\delta^2\Phi}{\delta J_{1'2'}\delta J_{3'4'}}\right)^0+J^z_{2'1'}J^z_{4'3'}\left(\frac{\delta^2\Phi}{\delta J^z_{1'2'}\delta J^z_{3'4'}}\right)^0+2J_{2'1'}J^z_{4'3'}\left(\frac{\delta^2\Phi}{\delta J_{1'2'}\delta J^z_{3'4'}}\right)^0\right]+\frac{1}{3!}\cdots. \tag{3.1}$$

Here the notation using parantheses means that for the resulting variational derivatives both arguments, J and J^z, are regarded to be equal to zero.

Functional differentiation of Φ with respect to field J^z can be replaced by the one with respect to another field h by using the following coupling equations

$$\frac{\delta\Phi}{\delta J^z_{12}}=\frac{1}{2}\left(\frac{\delta^2\Phi}{\delta h_1\delta h_2}+\frac{\delta\Phi}{\delta h_1}\frac{\delta\Phi}{\delta h_2}\right), \tag{3.2}$$

$$\frac{\delta^2\Phi}{\delta J^z_{12}\delta J^z_{34}}=\frac{1}{4}\left(\frac{\delta^2}{\delta h_1\delta h_2}+\frac{\delta\Phi}{\delta h_1}\frac{\delta}{\delta h_2}+\frac{\delta\Phi}{\delta h_2}\frac{\delta}{\delta h_1}\right)\times\left(\frac{\delta^2\Phi}{\delta h_3\delta h_4}+\frac{\delta\Phi}{\delta h_3}\frac{\delta\Phi}{\delta h_4}\right), \tag{3.3}$$

etc., which arise from subsequent differentiation of Eq. (2.7). As a result, the coefficients of the Taylor series (3.1) appear only in the form of variational derivatives of Φ with respect to J and h. These derivatives are calculated by differentiating either Eq. (2.24) or the Taylor series (3.1), respectively. While making this derivation, one has to use Eqs. (2.25), (2.26) and the following identities

$$\frac{\delta k_{12}}{\delta h_3}=-k_{11'}\frac{\delta k^{-1}_{1'2'}}{\delta h_3}k_{2'2},\quad \frac{\delta k^{(0)}_{12}}{\delta h_3}=-k^{(0)}_{13}k^{(0)}_{32}; \tag{3.4}$$

$$\frac{\delta}{\delta J_{34}}\alpha_0(12;5)=\delta_{15}\delta_{14}\delta_{32}. \tag{3.5}$$

Let us apply this procedure and calculate $\langle S^z_1\rangle_V$ up to the second order in J and J^z. Substituting the Taylor expansion (3.1) into Eq. (2.19) one writes, up to the second order,

$$\langle S_1^z\rangle = \frac{\delta\Phi}{\delta h_1} = \frac{\delta\Phi_0}{\delta h_1} + J_{2'1'}\frac{\delta}{\delta h_1}\left(\frac{\delta\Phi}{\delta J_{1'2'}}\right)^0 + J^z_{2'1'}\frac{\delta}{\delta h_1}\left(\frac{\delta\Phi}{\delta J^z_{1'2'}}\right)^0 + \frac{1}{2!}\Bigg[J_{2'1'}J_{4'3'}\frac{\delta}{\delta h_1}\left(\frac{\delta^2\Phi}{\delta J_{1'2'}\delta J_{3'4'}}\right)^0$$

$$+ 2J_{2'1'}J^z_{4'3'}\frac{\delta}{\delta h_1}\left(\frac{\delta^2\Phi}{\delta J_{1'2'}\delta J^z_{3'4'}}\right)^0 + J^z_{2'1'}J^z_{4'3'}\frac{\delta}{\delta h_1}\left(\frac{\delta^2\Phi}{\delta J^z_{1'2'}\delta J^z_{3'4'}}\right)^0\Bigg] + \cdots. \tag{3.6}$$

Here the second, third, and the fifth terms equal zero due to the space locality of the zero-order GF, $k_{12}^{(0)} \sim \delta_{12}$, which is seen from Eq. (2.18), while the exchange integrals J_{ij} and J^z_{ij} do not possess that property. Further, the second derivative with respect to J is found by differentiating Eq. (2.24),

$$\left(\frac{\delta^2\Phi}{\delta J_{12}\delta J_{34}}\right)^0 = k_{14}^{(0)}\left(\frac{\delta\Phi}{\delta h_4}\right)^0 k_{32}^{(0)}\left(\frac{\delta\Phi}{\delta h_2}\right)^0 - k_{14}^{(0)}k_{34}^{(0)}k_{42}^{(0)}\left(\frac{\delta\Phi}{\delta h_2}\right)^0 - k_{12}^{(0)}k_{32}^{(0)}k_{24}^{(0)}\left(\frac{\delta\Phi}{\delta h_4}\right)^0 + (k_{12}^{(0)}k_{34}^{(0)} + k_{14}^{(0)}k_{32}^{(0)})\left(\frac{\delta^2\Phi}{\delta h_2\delta h_4}\right)^0. \tag{3.7}$$

In its turn, the remaining second derivative of Φ with respect to J^z can be expressed with the help of Eq. (3.3) in terms of different derivatives of Φ with respect to h having the space locality as well. Finally, one obtains

$$\langle S_1^z\rangle = \frac{\delta\Phi_0}{\delta h_1} + J^z_{2'1'}\left(\frac{\delta^2\Phi}{\delta h_1\delta h_{1'}}\right)^0\frac{\delta\Phi_0}{\delta h_{2'}} - k^{(0)}_{11'}\frac{\delta\Phi_0}{\delta h_{1'}}J_{1'2'}k^{(0)}_{2'3}\frac{\delta\Phi_0}{\delta h_{3'}}J_{3'4'}k^{(0)}_{4'1} + \left(\frac{\delta^2\Phi}{\delta h_1\delta h_{1'}}\right)^0(Jk^{(0)})_{1'2'}\frac{\delta\Phi_0}{\delta h_{2'}}(Jk^{(0)})_{21'}$$

$$+ J^z_{2'1'}J^z_{4'3'}\left[\frac{1}{2}\left(\frac{\delta^3\Phi}{\delta h_1\delta h_{1'}\delta h_{3'}}\right)^0\left(\frac{\delta^2\Phi}{\delta h_{2'}\delta h_{4'}}\right)^0 + \left(\frac{\delta^2\Phi}{\delta h_1\delta h_{1'}}\right)^0\frac{\delta\Phi_0}{\delta h_{3'}}\left(\frac{\delta^2\Phi}{\delta h_{2'}\delta h_{4'}}\right)^0 + \frac{1}{2}\frac{\delta\Phi_0}{\delta h_{1'}}\frac{\delta\Phi_0}{\delta h_{3'}}\left(\frac{\delta^3\Phi}{\delta h_1\delta h_{2'}\delta h_{4'}}\right)^0\right]$$

$$+ \cdots. \tag{3.8}$$

Hereafter the zero-order first derivative of Φ with respect to h is written as $\delta\Phi_0/\delta h_1$, where $\Phi_0(h)$ is the first term of the Taylor series (3.1).

The correspondence between particular elements contributing to perturbation series and their graphical representation is shown in Fig. 1. Graphical representation for the series (3.8) is shown in Fig. 2. First of all, note that particular graphs contain one or more identical single-tail parts. It can be argued that summation of infinite series of these graphs results merely in renormalization of the argument in $\Phi_0(h)$. More precisely, the external field h has to be replaced by an effective field $\tilde{h}$. Therefore, in the series for $\langle S_1^z\rangle$, all the graphs containing single-tail parts can be dropped with the replacement $h \to \tilde{h}$ being made.[4] The graphical series for $h \to \tilde{h}$ thus reduced is given in Fig. 3.

A series expansion for the longitudinal GF determined by Eq. (2.21) can be found by taking the h derivative of the series (3.8). Differentiation of $k_{12}^{(0)}$ with respect to h should be performed with the help of Eq. (3.4), while differentiation of Φ merely raises up a derivative order. This results in the following series expansion where the single-tail parts are omitted,

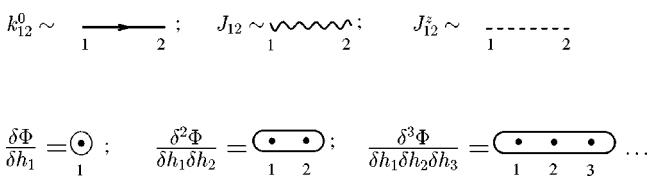

FIG. 1. Graphical representation of the basic elements of the diagrammatic technique for spin operators.

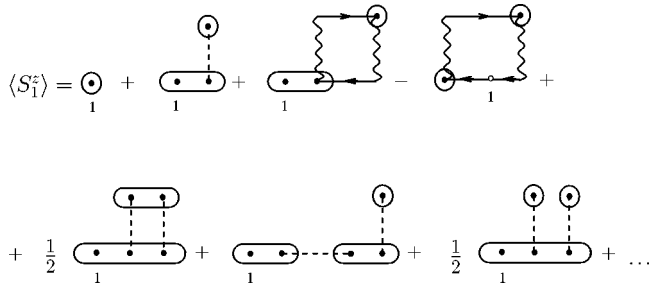

FIG. 2. Graphical representation of the perturbation expansion of the average spin $\langle S_1^z\rangle$.

$$\langle TS_1^z S_2^z\rangle_c = \frac{\delta^2\Phi_0}{\delta h_1 \delta h_2} + J^z_{2'1'}\left(\frac{\delta^2\Phi}{\delta h_1 \delta h_{1'}}\right)^0\left(\frac{\delta^2\Phi}{\delta h_2 \delta h_{2'}}\right)^0 + \left(k^{(0)}\frac{\delta\Phi_0}{\delta h}Jk^{(0)}\right)_{12}\left(k^{(0)}\frac{\delta\Phi_0}{\delta h}Jk^{(0)}\right)_{21}$$
$$+ k^{(0)}_{12}\left(k^{(0)}\frac{\delta\Phi_0}{\delta h}Jk^{(0)}\frac{\delta\Phi_0}{\delta h}Jk^{(0)}\right)_{21} + \left(k^{(0)}\frac{\delta\Phi_0}{\delta h}Jk^{(0)}\frac{\delta\Phi_0}{\delta h}Jk^{(0)}\right)_{12}k^{(0)}_{21}$$
$$- \left(k^{(0)}\frac{\delta\Phi_0}{\delta h}Jk^{(0)}\right)_{11'}\left(\frac{\delta^2\Phi}{\delta h_2 \delta h_{1'}}\right)^0 (Jk^{(0)})_{1'1} - \left(\frac{\delta^2\Phi}{\delta h_1 \delta h_{1'}}\right)^0 (Jk^{(0)})_{1'2}\left(k^{(0)}\frac{\delta\Phi_0}{\delta h}Jk^{(0)}\right)_{21'},$$
$$- k^{(0)}_{11'}\left(\frac{\delta^2\Phi}{\delta h_2 \delta h_{1'}}\right)^0\left(Jk^{(0)}\frac{\delta\Phi_0}{\delta h}Jk^{(0)}\right)_{1'1} - \left(\frac{\delta^2\Phi}{\delta h_1 \delta h_{1'}}\right)^0\left(Jk^{(0)}\frac{\delta\Phi_0}{\delta h}Jk^{(0)}\right)_{1'2}k^{(0)}_{21'}$$
$$+ \left(\frac{\delta^2\Phi}{\delta h_1 \delta h_{1'}}\right)^0 (Jk^{(0)})_{1'2'}\left(\frac{\delta^2\Phi}{\delta h_2 \delta h_{2'}}\right)^0 (Jk^{(0)})_{2'1'} + \frac{\delta^3\Phi}{\delta h_1 \delta h_2 \delta h_{1'}}(Jk^{(0)})_{1'2'}\left(\frac{\delta\Phi_0}{\delta h_{2'}}\right)(Jk^{(0)})_{2'1'}$$
$$+ J^z_{2'1'}J^z_{4'3'}\left[\left(\frac{\delta^2\Phi}{\delta h_1 \delta h_{1'}}\right)^0\left(\frac{\delta^2\Phi}{\delta h_2 \delta h_{3'}}\right)^0\left(\frac{\delta^2\Phi}{\delta h_{2'} \delta h_{4'}}\right)^0 + \frac{1}{2}\left(\frac{\delta^4\Phi}{\delta h_1 \delta h_2 \delta h_{4'} \delta h_{3'}}\right)^0\left(\frac{\delta^2\Phi}{\delta h_{2'} \delta h_{4'}}\right)^0\right.$$
$$\left. + \frac{1}{2}\left(\frac{\delta^3\Phi}{\delta h_1 \delta h_{1'} \delta h_{3'}}\right)^0\left(\frac{\delta^3\Phi}{\delta h_{4'}}\right)^0\right] + \cdots . \tag{3.9}$$

The graphical representation for this series is shown in Fig. 4.

By acting in a very similar manner, one can find the corresponding analytic series expansion for the transverse GF and its graphical representation, which we omit for the sake of brevity. Comparative analysis of the derived graphical series shows that each nth order term contains $2n$ internal vertices joined by propagator (Green) lines, cumulants (which correspond to variational derivatives of Φ with respect to h) and lines of interactions. External vertices (i.e., the ones without attached lines of interactions) correspond to spin operators S_1^z, S_1^-, and S_1^+ entering into the definitions of GFs. General rules for constructing particular diagrams are summarized below.

(1) There are two sorts of the S^z-type vertices: (a), without attached Green's lines and (b), with one incoming and one outgoing Green's lines. There is one sort of the S^--type vertices (c), with one outgoing Green's line, while two sorts of the S^+-type vertices are present: either (d), with one incoming Green's line or (e), with two incoming and one outgoing Green lines, (see Fig. 5).

(2) Internal vertices are joined by lines of interaction in such a way that the vertices of the S^z type are connected by dashed lines, whereas vertices of the S^- type are connected with vertices of the S^+ type by wavy lines; see Fig. 6. There are no other joined vertices.

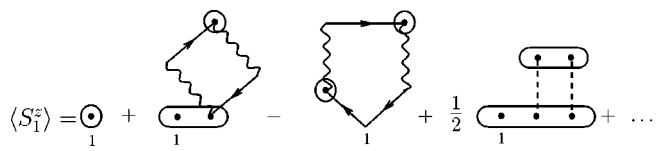

FIG. 3. Graphical representation of the resulting perturbation series of $\langle S_1^z\rangle$ after introducing the self-consistent field $\tilde{h}$.

(3) The sign of a particular diagram is determined by the parity (even/odd) of the total number of all "anomalous" vertices the diagram contains. The S^z-type vertices of the sort (b) and the S^+-type vertices of the sort (e) are regarded as anomalous ones. A fractional factor is determined by the permutation of the graph elements that do not change the diagram. This factor takes on the form $1/(n_a!n_b!\cdots)$ where n_a, n_b, . . . are the numbers of these permutations of sorts a, b, ...

One can see that the rules (1)–(3) coincide with those

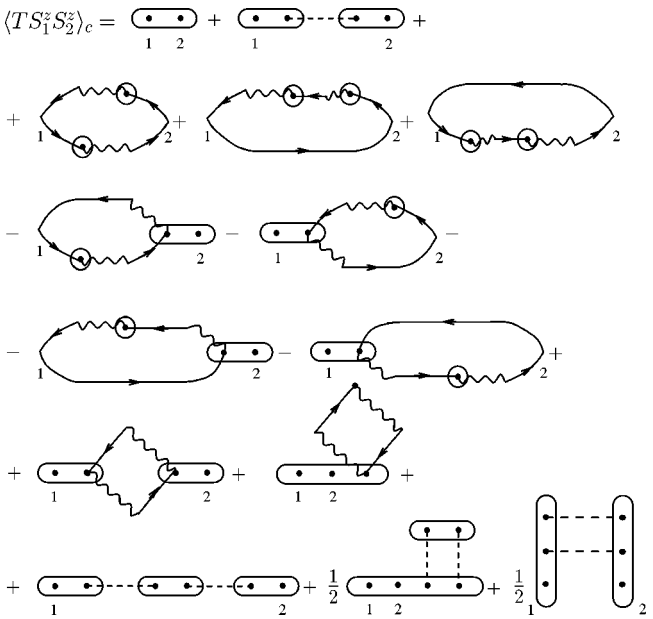

FIG. 4. Graphical representation of the longitudinal spin Green function.

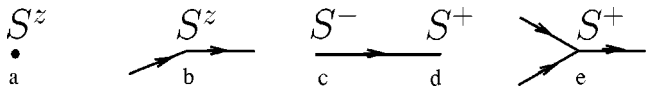

FIG. 5. The types of vertices in the Heisenberg model.

introduced many years ago[14,15] on the basis of the Wick theorem, which handles the contractions of the *T*-ordered operator products. In the present approach, instead, we exploit a set of equations in terms of variational derivatives of the generating functional $\Phi[h,J,J^z]$. Here, different contributions to the quantity under consideration are generated via the procedure of functional differentiation. Thus, if the standard approach takes account of a particular contribution by exhaustion of all possible operator pair contractions, the present approach deals with differentiation of products of the zero-order GFs. Within this automatic procedure, any term could be hardly lost. Moreover, when applying the present method, the topologically equivalent diagrams do not arise; their total contribution is taken into account automatically.

Note, since we consider an anisotropic Heisenberg model (2.1), two distinct lines of interaction are introduced to distinguish longitudinal and transverse spin components. Such a specification being a formal one permits us to better understand the structure of the perturbation series. By disregarding the difference between the dashed and wavy lines of interaction, one restores precisely the same graphical series that occur in the standard approach.

IV. LARKIN EQUATION. DIAGRAM SUMMATION

In the previous sections, the series expansions for the average spin $\langle S_1^z \rangle$ and the longitudinal GF, $\langle TS_1^z S_2^z \rangle$, were derived together with their graphical representations. To calculate the transverse GF, $\langle TS_1^- S_2^+ \rangle$, we derived Eqs. (2.25), (2.26) or the equivalent pair of equations (2.28), (2.26) for the self-energy part and the terminal part, respectively. By combining Eqs. (2.28), (2.26), one can check that the self-energy part M can be written as

$$M_{12} = m_{12} + P_{11'} J_{1'2}. \tag{4.1}$$

In terms of the diagrammatic technique, the quantity m_{12} should be called the part ''uncuttable'' across a line of interaction J_{12}. All the ''cuttable'' parts are compressed into the second term of the right-hand side of Eq. (4.1).

A close inspection of Eq. (2.24) shows that this equation can be also rewritten in the form

$$K_{12} = \Sigma_{12} + \Sigma_{11'} J_{1'2'} K_{2'2}, \tag{4.2}$$

where the notation (2.3) for the transverse GF is used, and the quantity Σ_{12} is defined as

$$\Sigma_{12} = (k^{ir} P)_{12}, \quad (k^{ir})_{12}^{-1} = k_{12}^{(0)-1} - m_{12}.$$

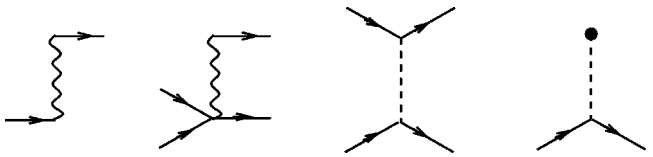

FIG. 6. Bare vertex parts in the Heisenberg model.

Evidently, the part Σ_{12} is ''uncuttable'' across a line of interaction and, hence, Eq. (4.2) is the Larkin equation derived earlier (see, for instance, Ref. 16) in the framework of the diagrammatic technique for the spin operators.[4] With the use of the equation of motion for the longitudinal GF it can be shown that this GF obeys also the Larkin equation

$$D_{12}^z = \Sigma_{12}^z + \Sigma_{11'}^z J_{1'2'}^z D_{2'2}^z, \tag{4.3}$$

where Σ_{12}^z denotes the set of diagrams that cannot be cut across a line of interaction J_{12}^z. Consequently, we have a complete coincidence of the generating functional formalism and the standard diagrammatic technique.

Let us now turn back to Eqs. (2.26), (2.28) to calculate the transverse GF. These equations being iterated lead to power series in interaction. Up to the second order of J, we obtain the following series expansions

$$\begin{aligned} M_{12} = {} & \alpha_0(12;4') \frac{\delta \Phi}{\delta h_{4'}} - \alpha_0(12';2) k_{2'2} \\ & + \alpha_0(12';4') k_{2'3} \alpha_0(3'2;6') \frac{\delta^2 \Phi}{\delta h_{4'} \delta h_{6'}} \\ & + \alpha_0(12';4') k_{2'3'} \alpha_0(3'1';2) k_{1'4'} k_{4'2} + \cdots, \end{aligned} \tag{4.4}$$

$$\begin{aligned} P_{12} = {} & \alpha_0(11';2') \frac{\delta^2 \Phi}{\delta h_{2'} \delta h_2} k_{1'2} \\ & - k_{4'1'} \alpha_0(13';2') \alpha_0(1'4';6') \frac{\delta^2 \Phi}{\delta h_{2'} \delta h_2} k_{3'6'} k_{6'2} \\ & + k_{4'1'} \alpha_0(14';6') \alpha_0(1'3';2') \frac{\delta^3 \Phi}{\delta h_{2'} \delta h_{6'} \delta h_2} k_{3'2} \\ & + \cdots. \end{aligned} \tag{4.5}$$

The terms of these series expansions contain exact propagator functions k and many-particle GFs of the longitudinal spin components. Each of them has to be calculated separately by using some appropriate approximations.

After writing the expression (2.14) for α_0 explicitly, the series take on the following forms:

$$M_{12}=\frac{\delta\Phi}{\delta h_1}J_{12}-\delta_{12}J_{12'}\frac{\delta\Phi}{\delta h_{2'}}-\delta_{12}(Jk)_{11}+J^z_{12}k_{12}$$
$$+J_{12'}\frac{\delta^2\Phi}{\delta h_1\delta h_{3'}}k_{2'3'}J_{3'2}-J_{12'}k_{2'2}J^z_{23'}\frac{\delta^2\Phi}{\delta h_1\delta h_{3'}}$$
$$-J^z_{12'}k_{12}\frac{\delta^2\Phi}{\delta h_{2'}\delta h_{3'}}k_{13'}J_{3'2}+J^z_{12'}k_{12}\frac{\delta^2\Phi}{\delta h_{2'}\delta h_{3'}}$$
$$\times J^z_{23'}-J_{12'}k_{2'2}J_{23'}k_{3'1}k_{12}-J_{12'}k_{2'1}J^z_{1'2}k_{1'1}k_{12}$$
$$-J^z_{12'}k_{12}J_{23'}k_{3'2'}k_{2'2}+J^z_{12'}k_{2'2}k_{13'}J^z_{3'2}k_{3'2'}+\cdots \tag{4.6}$$

$$P_{12}=\delta_{12}\frac{\delta\Phi}{\delta h_2}+(Jk)_{12}\frac{\delta^2\Phi}{\delta h_1\delta h_2}-k_{12}J^z_{12'}\frac{\delta^2\Phi}{\delta h_{2'}\delta h_2}+\cdots \tag{4.7}$$

(where the last expression is shortened for the sake of brevity), and their graphical representations are depicted in Fig. 7. We adopt a convention that the exact GF, k_{12}, is given by a thick line, whereas k^0_{12} is presented by a thin line. A direct inspection shows that the graphs representing M and P (Fig. 7) satisfy all the rules of the diagrammatic technique based on the Wick theorem.

Let us now write down the Fourier transformed, $q=\{\mathbf{q},i\omega_n\}$, second-order correction to the self-energy part,

$$M^{(2)}_q=\sum_{k_1}(J_{\mathbf{q}+\mathbf{k}_1}-J^z_{\mathbf{k}_1})(J_{\mathbf{q}}-J^z_{\mathbf{k}_1})k(q+k_1)D(k_1)$$
$$-\sum_{k_1k_2}(J_{\mathbf{k}_1}-J^z_{\mathbf{k}_1-\mathbf{q}})(J^z_{\mathbf{k}_2-\mathbf{q}}-J_{\mathbf{k}_1+\mathbf{k}_2-\mathbf{q}})$$
$$\times k(k_1)k(k_2)k(k_1+k_2-q). \tag{4.8}$$

Here $k(k)$ and $D(k)$ are the Fourier transforms of the transverse GF, $\langle TS^-_1S^+_2\rangle$, and the longitudinal GF, $\langle TS^z_1S^z_2\rangle$, respectively. The transverse GF is calculated in the Hartree-Fock approximation that gives

$$k(q)\equiv k_{\mathbf{q}}(i\omega_n)=\frac{1}{i\omega_n+\varepsilon_{\mathbf{q}}},\quad \omega_n=2\pi nT. \tag{4.9}$$

This GF describes propagation of a spin wave with the momentum $\mathbf{q}$ and energy

$$\varepsilon_{\mathbf{q}}=\langle S^z\rangle(J_{\mathbf{0}}-J_{\mathbf{q}}). \tag{4.10}$$

In the series for the longitudinal GF (Fig. 4) one has to thicken up the elementary Green line within the Hartree-Fock approximation. Then the graphs in Fig. 4 are transformed to those shown in Fig. 8 which contains the thick Green lines of spin waves. The zero-order expression for D (however, with the dressed transverse GF) is given by the following form of $\Sigma^z(q)$ that is a sum of two contributions

$$\Sigma^z(q)\equiv\Sigma^z_{\mathbf{q}}(i\omega_n)=b'\delta_{\omega_n0}+\Pi(q), \tag{4.11}$$

where

$$\Pi(q)\equiv\sum_k k(k)k(k-q) \tag{4.12}$$

is the expression for the loop graph describing a contribution of spin waves to longitudinal spin components fluctuations; b' being the first derivative of the Brillouin function corresponds to the first graph in Fig. 8.

First and second terms in Eq. (4.11) describe static and dynamic fluctuations, respectively. Taking into account only the dynamic contribution $D(q)\approx\Sigma^z_q=\Pi_q$ after its substitution into Eq. (4.8), one sees that both terms in the right-hand side of Eq. (4.11) acquire the same structure. Combining both the terms into one and summing up over frequencies, we obtain the self-energy correction to spin waves[4,15,20]

$$M^{(2)}_{\mathbf{q}}(i\omega_n)$$
$$=\frac{1}{2N^2}\sum_{\mathbf{k}_1\mathbf{k}_2}(J^z_{\mathbf{k}_1-\mathbf{q}}+J^z_{\mathbf{k}_2-\mathbf{q}}-J_{\mathbf{k}_1}-J_{\mathbf{k}_2})$$
$$\times(J^z_{\mathbf{k}_1-\mathbf{q}}+J^z_{\mathbf{k}_2-\mathbf{q}}-J_{\mathbf{k}_1+\mathbf{k}_2-\mathbf{q}}-J_{\mathbf{q}})$$
$$\times\frac{n(\varepsilon_{\mathbf{k}_1+\mathbf{k}_2-\mathbf{q}})[1+n(\varepsilon_{\mathbf{k}_1})+n(\varepsilon_{\mathbf{k}_2})]-n(\varepsilon_{\mathbf{k}_1})n(\varepsilon_{\mathbf{k}_2})}{i\omega_n-\varepsilon_{\mathbf{k}_1}-\varepsilon_{\mathbf{k}_2}+\varepsilon_{\mathbf{k}_1+\mathbf{k}_2-\mathbf{q}}}. \tag{4.13}$$

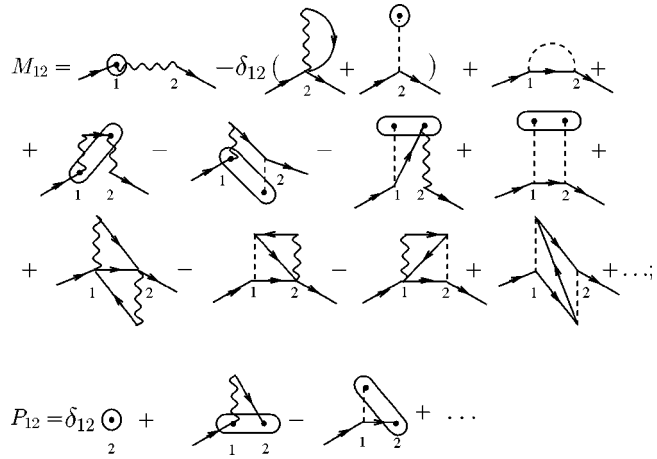

FIG. 7. The self-energy and terminal parts of the transverse spin Green function.

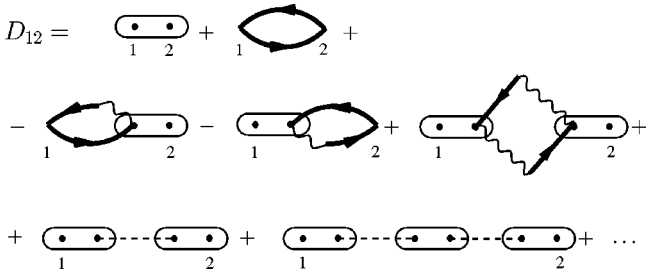

FIG. 8. The longitudinal spin Green function with spin-wave Green function lines shown by thick solid lines.

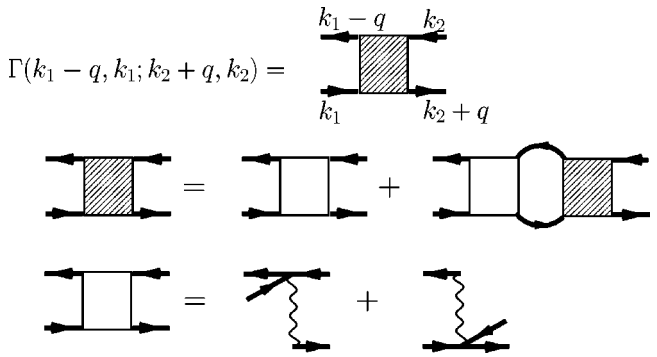

FIG. 9. The effective four-point part with the equation it obeys.

Here each linear combination of four $J_{\mathbf{q}}$ is an amplitude of a two-spin-wave interaction. Analysis of this expression for the spin-wave self-energy correction allows us to conclude that in accordance with VLP spin waves are weakly damped in the long-wavelength limit for all $T<T_C$. For antiferromagnets similar results were obtained in the fundamental paper.[21]

V. GREEN FUNCTION FOR LONGITUDINAL SPIN COMPONENTS

The longitudinal GF,

$$D_{12}=\langle T(S_1^z-\langle S_1^z\rangle)(S_2^z-\langle S_2^z\rangle)\rangle, \tag{5.1}$$

could be calculated by deriving and solving new equations in terms of variational derivatives as was done previously for the transverse GF. Instead, in this section we carry out calculations by relying on the diagrammatic technique developed in Secs. III and IV. For instance, the diagrammatic series for the longitudinal GF is presented in Fig. 4. There the thickening of spin-wave lines that results from the Hartree-Fock approximation leads to a simpler graphical series, Fig. 8. Only the graphs of zero, first, and second order in interaction are shown. Already an analysis of these low-order terms shows that D_{12} includes four distinct loops with antiparallel Green lines, namely, a simple loop, a loop with two inserted wavy lines, and two different loops with one inserted wavy line. By using the rules of the diagrammatic technique, Sec. III, one can continue constructing the series and find that these four sorts of loops appear in arbitrary combinations in higher-order series terms.

Summation of this kind of diagrams can be made by using a method proposed earlier[18,19] in the framework of the diagrammatic technique elaborated for the t-J model. The central point of this method is a calculation of the four-point vertex Γ presented graphically in Fig. 9, which satisfies the Bethe-Salpeter equation (see Fig. 9). By applying an iteration procedure to this equation, one finds an infinite series of chainlike diagrams built out of four distinct loops described above. The graphical equation from Fig. 9 is expressed analytically as follows

$$\begin{aligned}\Gamma(k_1-q,k_1;k_2+q,k_2)&=J_{\mathbf{k}_2+\mathbf{q}}+J_{\mathbf{k}_1-\mathbf{q}}+\frac{1}{N}\sum_{\mathbf{k}_3}J_{\mathbf{k}_3}k(k_3-q)k(k_3)\\&\times\Gamma(k_3-q,k_3;k_2+q,k_2)\\&+J_{\mathbf{k}_1-\mathbf{q}}\frac{1}{N}\sum_{\mathbf{k}_3}k(k_3-q)k(k_3)\Gamma(k_3-q,k_3;k_2+q,k_2).\end{aligned} \tag{5.2}$$

Here $k(q)$ is the propagator (4.9) of a spin wave with the momentum $\mathbf{q}$ and Matsubara frequency $\omega_n=2n\pi T$, and we use the notation $q=\{\mathbf{q},i\omega_n\}$. Since the integral equation (5.2) has a degenerate kernel, it can be transformed to an algebraic form. To this end, let us first multiply Eq. (5.2) by $k(k_1-q)k(k_1)$ and sum up both sides of it over k_1. In addition, Eq. (5.2) is multiplied by $J_{\mathbf{k}_1}k(k_1-q)k(k_1)$ and, consequently, summed up over k_1. This results in a set of two linear equations with the solution

$$\begin{aligned}\Gamma(k_1-q,k_1;k_2+q,k_2)&=\frac{1}{d(q)}\{\Phi(q)+J_{\mathbf{k}_1-\mathbf{q}}[1-Q(q)]+J_{\mathbf{k}_2+\mathbf{q}}[1-\Lambda(q)]\\&+J_{\mathbf{k}_1-\mathbf{q}}J_{\mathbf{k}_2+\mathbf{q}}\Pi(q)\},\end{aligned} \tag{5.3}$$

where

$$d(q)=[1-\Lambda(q)][1-Q(q)]-\Pi(q)\Phi(q). \tag{5.4}$$

The last two expressions involve four quantities defined as

$$\begin{pmatrix}\Pi(q)\\Q(q)\\\Lambda(q)\\\Phi(q)\end{pmatrix}=\frac{1}{N}\sum_{k_1}\begin{pmatrix}1\\J_{\mathbf{k}_1}\\J_{\mathbf{k}_1-\mathbf{q}}\\J_{\mathbf{k}_1}J_{\mathbf{k}_1-\mathbf{q}}\end{pmatrix}k(k_1-q)k(k_1), \tag{5.5}$$

which correspond to four distinct loops appearing in the expansion series for the longitudinal GF (Fig. 8).

The loop approximation is further applied to calculate three-point vertices, γ_L and γ_R, shown graphically in Fig. 10 that correspond to the interaction of spin waves with longitudinal fluctuations. In accordance with the equations presented graphically in Fig. 10, and by taking into account the expression (5.3) for the four-point vertex, one obtains

$$\gamma_L(k_1-q,k_1;q)=\frac{1}{d(q)}\{\Phi(q)+J_{\mathbf{k}_1-\mathbf{q}}[1-Q(q)]\}, \tag{5.6}$$

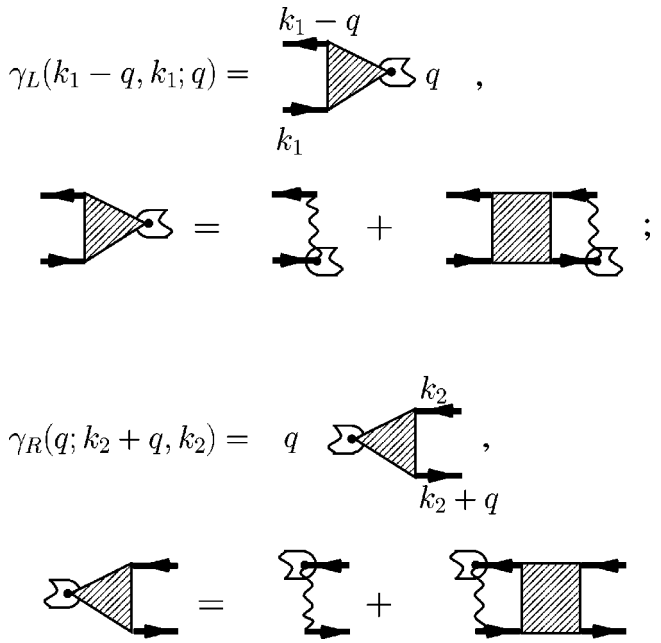

FIG. 10. Relation between three-point and four-point parts.

$$\gamma_R(q;k_2+k,q)=\frac{1}{d(q)}\{\Phi(q)+J_{\mathbf{k}_2+\mathbf{q}}[1-\Lambda(q)]\}. \tag{5.7}$$

The resulting expressions for the vertex parts Γ, γ_L, and γ_R are necessary to calculate the longitudinal GF, D_{12}.

We proceed considering the irreducible part Σ^z_{12} of D_{12} defined graphically in Fig. 11. Here the irreducibility is understood in the sense that Σ^z_{12} is represented by the collection of all diagrams from the series for D_{12} that cannot be cut across a line of interaction J^z. In Fig. 11, the first thickened element in the row denotes a ''dressed'' cumulant obeying the Dyson equation with an irreducible self-energy part m^z, (see Fig. 12). We call it the ''propagator'' k^z.

In Fig. 11, all the possible loop diagrams contributing to the longitudinal GF are depicted. There two external vertices of the GF labeled as 1 and 2 are represented both by two sorts of vertices: one is given by a thickened dot, and the second is a simple point with an incoming and an outgoing Green lines. Other arrangements of external vertices do not exist.

By using the notation $\pi(k)$ for the zero-order cumulant (the first term in the right-hand side of the Dyson equation represented graphically in Fig. 12) and recalling that[4,22]

$$\pi(q)=b'\,\delta_{\omega_n 0}, \tag{5.8}$$

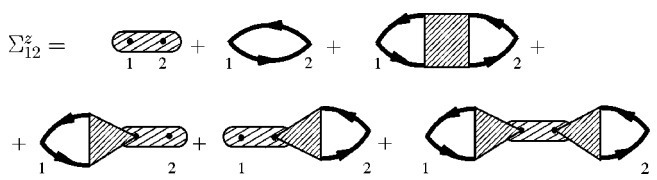

FIG. 11. The complete self-energy part of the longitudinal spin Green function.

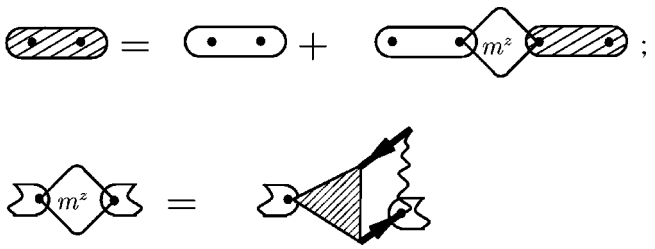

FIG. 12. The equation for the ''dressed'' second-order cumulant.

one obtains from the graphical equation (Fig. 12), the following analytic expression for the ''propagator''

$$k^z(q)=\frac{b'\,\delta_{\omega_n 0}}{1-b'm^z(q)}, \tag{5.9}$$

where

$$m^z(q)=\frac{\Phi(q)}{d(q)}. \tag{5.10}$$

Returning to Fig. 11, note that, for instance, the total contribution of the second and third graphs there are given by

$$\Pi(q)+\frac{1}{N^2}\sum_{k_1k_2}k(k_1-q)k(k_1)\Gamma(k_1-q,k_1;k_2+q,k_2)$$
$$\times k(k_2)k(k_2+q)=\frac{\Pi(q)}{d(q)}, \tag{5.11}$$

and the other contributions can be found and expressed in the same way. By summing up all the contributions we obtain

$$\Sigma^z(q)=\frac{\pi(q)+\Pi(q)}{[1-\Lambda(q)][1-Q(q)]-[\pi(q)+\Pi(q)]\Phi(q)}. \tag{5.12}$$

In the final step one has to take into account all the graphs with lines of interaction J^z connecting the irreducible elements in Σ^z_{12}, Fig. 11. The problem is reduced to searching for a solution of the Larkin equation (4.3) where Σ^z_{12} is given by Eq. (5.12). That leads us to the final expression for the longitudinal GF,

$$D(q)=\frac{\pi(q)+\Pi(q)}{[1-\Lambda(q)][1-Q(q)]-[\pi(q)+\Pi(q)][\Phi(q)+J^z_{\mathbf{q}}]}. \tag{5.13}$$

Thus, the inclusion of all the graphs with lines of interaction J^z amounts to the replacement, $\Phi(q)\to\Phi(q)+J_{\mathbf{q}}$, in Eq. (5.12) if one compares this expression with the complete result, Eq. (5.13).

A similarity between the present result and that obtained in the study of the t-J model[18,19] has been briefly mentioned in Introduction. Some more comments are worth making. Actually, the expression (5.12) derived for the longitudinal GF has the same structure as that for the spin GFs (longitu-

dinal and transverse ones) obtained for the t-J model.[18,19] A formal difference is that instead of $J^z_{\mathbf{q}}$, the Fourier transform $t_{\mathbf{q}}$ for the intersite electron hopping integral occurs in the case of the t-J model. What is more, if the bosoniclike loops Π, Λ, Q, and Φ enter into Eq. (5.13), then analogous fermioniclike ones appear in the corresponding expression obtained in the t-J model. Beyond these formal differences, a remarkable similarity among two groups of results, first, is caused by the close resemblance of corresponding diagrammatic series arising in both the models and, second, is due to a common character of the approximation (a summation of all loop-type diagrams) used. Therefore, like in the case of the t-J model, the approximation employed here in the derivation of the longitudinal GF is of the GRPA type. In contrast to this, GRPA is useless, however, while treating in the framework of the Heisenberg model the transverse spin GF, since a summation, for instance, of the ladder diagrams is required in this case. We note also that GRPA is the first-order approximation with respect to the parameter $1/z$ (z is the first coordination number of a lattice) that enters through Π, Λ, Q, and Φ into the denominator of Eq. (5.13) and, thus, determines the poles and other singular properties of this GF. In this respect, these three loops are equally important, and none of them can be ignored.

Note that the expression (5.13) contains a singular discrete frequency part $\delta_{\omega_n 0}$ coming from the quantity $\pi(q) = b' \delta_{\omega_n 0}$. This quantity corresponds to a single-site zero-order cumulant and, thus, does not depend on the thermodynamic time. This singular contribution to the temperature Green function arises due to the distinction between the isolated and isothermal susceptibilities of the system. This problem was studied in the general form in Refs. 23 and 24 and for a particular model with interaction of lattice vibrations with two-level defects.[25] First, we separate the singular contribution in the general expression (5.13) writing it in the form

$$D(\mathbf{q}, i\omega_n) = D^I(\mathbf{q}, i\omega_n) + \delta_{\omega_n,0}[D^T(\mathbf{q},0) - D^I(\mathbf{q},0)], \tag{5.14}$$

where

$$D^I(\mathbf{q}, i\omega_n) \equiv D^I(q) = \frac{\Pi(q)}{[1-\Lambda(q)][1-Q(q)] - \Pi(q)[\Phi(q) + J^z_{\mathbf{q}}]}, \tag{5.15}$$

$$D^T(\mathbf{q},0) = \frac{b' + \Pi(\mathbf{q},0)}{[1-\Lambda(\mathbf{q},0)][1-Q(\mathbf{q},0)] - [b' + \Pi(\mathbf{q},0)][\Phi(\mathbf{q},0) + J^z_{\mathbf{q}}]}. \tag{5.16}$$

The intensity of the singular contribution coincides with the distinction between the isothermal D^T and isolated D^I susceptibilities at the zeroth frequency. In accordance with the general analysis of different susceptibilities,[23,24] the distinction between them points to the nonergodicity of the system.

We will be interested in the isolated (Kubo) susceptibility of the system derived from the quantity $D^I(\mathbf{q}, i\omega_n)$ (5.15) by analytic continuation from the Matsubara frequencies onto the real axis $i\omega_n \to \Omega + i\delta$. To calculate the dependence of the spin susceptibility $\chi^{zz}(\mathbf{q}, i\omega_n)$ with the relation (5.15), it is necessary to calculate the four quantities $\Pi(q), \Lambda(q)$, $Q(q)$, and $\Phi(q)$ given by formulas (5.5).

VI. CALCULATION OF THE LOOP DIAGRAMS

To calculate the loop diagrams $\Pi(q), \Lambda(q)$, $Q(q)$, and $\Phi(q)$, where $q = \{\mathbf{q}, i\omega_n\}$, let us substitute the spin-wave GF (4.9) into Eq. (5.5) and sum up over the discrete Matsubara frequencies, which gives

$$\begin{pmatrix} \Pi(q) \\ Q(q) \\ \Lambda(q) \\ \Phi(q) \end{pmatrix} = -\frac{1}{N} \sum_{\mathbf{k}} \begin{pmatrix} 1 \\ \varepsilon(\mathbf{k}) \\ \varepsilon(\mathbf{k}-\mathbf{q}) \\ \varepsilon(\mathbf{k})\varepsilon(\mathbf{k}-\mathbf{q}) \end{pmatrix} \frac{n(\varepsilon_{\mathbf{k}+\mathbf{q}}) - n(\varepsilon_{\mathbf{k}})}{i\omega_n - \varepsilon_{\mathbf{k}+\mathbf{q}} + \varepsilon_{\mathbf{k}}}, \tag{6.1}$$

where $n(\varepsilon_{\mathbf{k}})$ is the Bose distribution function for spin waves. Due to the property

$$\Lambda(-q) = Q(q), \quad \Pi(-q) = \Pi(q), \quad \Phi(-q) = \Phi(q), \tag{6.2}$$

the longitudinal GF (5.13) is an even one, $D(-q) = D(q)$, as well. Hereinafter we suppose that the analytic continuation $i\omega_n \to \Omega + i\delta$ is made in Eq. (6.1).

With a simple algebra, the quantities on the left-hand side of Eq. (6.1) can be expressed in terms of an universal function λ_α, ($\alpha = 0,1,2$) and an additional function ψ_α defined as

$$\lambda_\alpha(\mathbf{q}, \Omega) = \frac{1}{N} \sum_{\mathbf{k}} \left(\frac{\varepsilon_{\mathbf{k}}}{\langle S^z \rangle} \right)^\alpha \frac{n(\varepsilon_{\mathbf{k}})}{\Omega + \varepsilon_{\mathbf{k}-\mathbf{q}} - \varepsilon_{\mathbf{k}} + i\delta}, \tag{6.3}$$

$$\psi_\alpha = \frac{1}{\langle S^z \rangle} \frac{1}{N} \sum_{\mathbf{k}} \left(\frac{\varepsilon_{\mathbf{k}}}{\langle S^z \rangle} \right)^\alpha n(\varepsilon_{\mathbf{k}}). \tag{6.4}$$

Then one can write

$$\Pi=\lambda_0^+ +\lambda_0^-,$$

$$Q=-\psi_0+\frac{\Omega}{\langle S^z\rangle}\lambda_0^+ +J_0(\lambda_0^+ +\lambda_0^-)-(\lambda_1^+ +\lambda_1^-),$$

$$\Phi=-2J_0\psi_0+2\psi_1+J_0\frac{\Omega}{\langle S^z\rangle}(\lambda_0^+ -\lambda_0^-)-\frac{\Omega}{\langle S^z\rangle}(\lambda_1^+ -\lambda_1^-)$$
$$+J_0^2(\lambda_0^+ +\lambda_0^-)-2J_0(\lambda_1^+ +\lambda_1^-)+(\lambda_2^+ +\lambda_2^-),$$

where a shorthand notation $\lambda_\alpha^\pm=\lambda_\alpha(\mathbf{q},\pm\Omega)$ is used. Then the real part $\lambda'_\alpha(\mathbf{q},\Omega)$ is defined by Eq. (6.3) implying that its principal value has to be taken for this case. Hence, the imaginary part $\lambda''_\alpha(\mathbf{q},\Omega)$ reads

$$\lambda''_\alpha(\mathbf{q},\Omega)=-\pi\frac{1}{N}\sum_{\mathbf{k}}\left(\frac{\varepsilon_{\mathbf{k}}}{\langle S^z\rangle}\right)^\alpha n(\varepsilon_{\mathbf{k}})\,\delta(\Omega+\varepsilon_{\mathbf{k}-\mathbf{q}}-\varepsilon_{\mathbf{k}}). \tag{6.5}$$

The main physics can be captured by using the quadratic spin-wave dispersion

$$\varepsilon_{\mathbf{k}}=\langle S^z\rangle Jk^2, \tag{6.6}$$

when evaluating the quantities defined by Eqs. (6.3)–(6.5). Integration over the angle θ, formed of the momentum $\mathbf{k}$ with $\mathbf{q}$, leads us to an intermediate result

$$\lambda'^{\pm}_\alpha=\frac{\pi}{8}\frac{1}{J^{1-\alpha}}\frac{1}{\langle S^z\rangle q}f'_\alpha(a^\pm), \tag{6.7}$$

where

$$f'_\alpha(a)=\frac{\langle S^z\rangle}{2t}\int_0^1 dx\frac{x^{2\alpha+1}}{e^{(\langle S^z\rangle/t)x^2}-1}\ln\left|\frac{x+a}{x-a}\right| \tag{6.8}$$

and, analogously for the imaginary part (6.5), we obtain

$$\lambda''^{\pm}_\alpha=\mp\frac{\pi^2}{8}\frac{1}{J^{1-\alpha}}\frac{1}{\langle S^z\rangle q}f''_\alpha(a^\pm), \tag{6.9}$$

where

$$f''_\alpha(a)=\frac{\langle S^z\rangle}{2t}\int_{|a|}^1 dx\frac{x^{2\alpha+1}}{e^{(\langle S^z\rangle/t)x^2}-1} \tag{6.10}$$

if $|a|<1$, and $f''_\alpha(a)=0$ if $|a|>1$. Here $t=T/J$ is the dimensionless temperature, and the argument a in the expressions (6.7)–(6.10) is defined as

$$a^\pm=\frac{q}{2}\pm\frac{\omega}{2\langle S^z\rangle q}, \tag{6.11}$$

thus being a function of $\mathbf{q}$ and ω, ($\omega=\Omega/J$). One sees that the $(\omega,\mathbf{q})$ dependence of the longitudinal GF is described by two integrals, $f'_\alpha(a)$ and $f''_\alpha(a)$, which show even and odd symmetry in a, respectively.

Below we estimate both integrals, $f'_\alpha(a)$ and $f''_\alpha(a)$, for the high-temperature regime where the magnetization $\langle S^z\rangle$ is small, and, hence, $\langle S^z\rangle/t\ll 1$ holds. Under this condition, one gets, from Eq. (6.4), an estimate,

$$\psi_0\approx\frac{\pi}{2}\frac{t}{\langle S^z\rangle^2}. \tag{6.12}$$

When $|a|\ll 1$, the required asymptotic expansions are found to be

$$f'_0(a)=\frac{\pi^2}{4}\operatorname{sgn}a-a+\cdots,$$

$$f'_1(a)=a+\cdots,\quad f'_2(a)=\frac{1}{3}a+\cdots \tag{6.13}$$

for $f'_\alpha(a)$, and

$$f''_0(a)=\frac{1}{2}\ln\frac{1}{|a|}+\cdots,$$

$$f''_1(a)=\frac{1}{2}(1-a^2)+\cdots,\quad f''_2(a)=\frac{1}{4}(1-a^4)+\cdots \tag{6.14}$$

for $f''_\alpha(a)$.

Thus, if $|a|\ll 1$ holds, $f'_0(a)$ and $f''_0(a)$ are the leading terms in the expansions (6.13) and (6.14) and, hence, the terms with $\alpha=1,2$ can be dropped when estimating loop contributions Λ, Q, and Φ. Then once the analytic continuation in Eq. (5.15) is made, the longitudinal spin susceptibility reads

$$\chi^{zz}(\mathbf{q},\omega)=\frac{4\langle S^z\rangle^2}{\pi Tq}\frac{N'(\mathbf{q},\omega)+iN''(\mathbf{q},\omega)}{D'(\mathbf{q},\omega)+iD''(\mathbf{q},\omega)}, \tag{6.15}$$

where

$$N'=f_0^{+\prime}+f_0^{-\prime},\quad N''=-\pi(f_0^{+\prime\prime}-f_0^{-\prime\prime}), \tag{6.16}$$

$$D'=\left[f_0^{+\prime}\frac{\omega}{\langle S^z\rangle q}-\frac{4\langle S^z\rangle^2}{\pi t}(1+\psi_0)\right]\left[f_0^{-\prime}\frac{\omega}{\langle S^z\rangle q}+\frac{4\langle S^z\rangle^2}{\pi t}(1+\psi_0)\right]+\frac{12z}{\pi}\frac{\langle S^z\rangle^2}{tq}(f_0^{+\prime}+f_0^{-\prime})+\pi^2 f_0^{+\prime\prime}f_0^{-\prime\prime}\left(\frac{\omega}{\langle S^z\rangle q}\right)^2, \tag{6.17}$$

$$D''=-(f_0^{+\prime\prime}-f_0^{-\prime\prime})12z\frac{\langle S^z\rangle^2}{Tq}-\pi f_0^{-\prime\prime}\frac{\omega}{\langle S^z\rangle q}\left[f_0^{+\prime}\frac{\omega}{\langle S^z\rangle q}-\frac{4}{\pi}\frac{\langle S^z\rangle^2}{t}(1+\psi_0)\right]-\pi f_0^{+\prime\prime}\frac{\omega}{\langle S^z\rangle q}\left[f_0^{-\prime}\frac{\omega}{\langle S^z\rangle q}+\frac{4}{\pi}\frac{\langle S^z\rangle^2}{t}(1+\psi_0)\right]. \tag{6.18}$$

VII. SPECTRAL DENSITY OF LONGITUDINAL SPIN FLUCTUATIONS

It is instructive first to calculate the spectral density starting with the approximate solution for the longitudinal GF of Ref. 4, i.e., with $D_{SW}(q) \approx \Pi(q)$. In this approximation, the spectral density

$$\mathrm{Im}\, D_{SW}(\mathbf{q},\omega) \approx \mathrm{Im}\, \Pi(\mathbf{q},\omega) = 2\pi \frac{t}{J} \frac{1}{\langle S^z \rangle^2 q} \ln \left| \frac{\omega + \varepsilon_{\mathbf{q}}}{\omega - \varepsilon_{\mathbf{q}}} \right| \tag{7.1}$$

exhibits weak resonances at spin-wave energies as it was noted in Ref. 4. Since beyond the critical region $\langle S^z \rangle^2 \sim (T_C - T)$, formula (7.1) shows an increase in the spectral density as $T \to T_C$ and $\mathbf{q} \to \mathbf{0}$. However, the complete expression (5.13) with the denominator involved describes a strong renormalization of the longitudinal spin fluctuations due to processes of virtual creation and annihilation of spin waves.

Let us examine Eq. (6.15) more closely. First of all, let us investigate whether the equation $D'(\mathbf{q},\omega)$ has solutions that would determine the dispersion law of longitudinal wave excitations. To this end, we make use of the analytic expansions (6.13) and (6.14) assuming that $|a| \ll 1$. It is not difficult to show that there indeed is a solution of that sort,

$$\omega_q \approx 0.43 \langle S^z \rangle q, \tag{7.2}$$

and the expansion parameter a does not go beyond the analytic region (6.13). The quantity ω_q should be considered as the frequency of collective vibrations of longitudinal components of the spin. It lies energetically above the spin-wave frequency $\varepsilon_q / J = \langle S^z \rangle q^2$ at the same temperature and wave vector.

The shape of the spectral density $\mathrm{Im}\, D(\mathbf{q},\omega)$ can be studied only numerically. We have two parameters dependent on temperature: t and $\langle S^z \rangle$. We take the temperature dependence of magnetization in the mean-field approximation,

$$\langle S^z \rangle = S\sqrt{1-\tau}, \quad \tau = T/T_C, \tag{7.3}$$

where T_C is the Curie point. To be not attached to a particular ferromagnetic model, we define T_C in the form $T_C = \upsilon S J$ where υ is a dimensionless parameter of an order of unity that should be calculated for a chosen model. Thus, all the temperature factors in the expressions (6.17) and (6.18) are written in terms of the relative temperature τ and model parameter υ,

$$\frac{\langle S^z \rangle}{t} = \frac{1}{\upsilon} \frac{\sqrt{1-\tau}}{\tau}, \quad \frac{\langle S^z \rangle^2}{t} = \frac{S}{\upsilon} \frac{1-\tau}{\tau}.$$

The $(\mathbf{q},\omega)$ dependence of the dynamic structure factor

$$S^{zz}(\mathbf{q},\omega) = \frac{J}{\omega} \mathrm{Im}\, D(\mathbf{q},\omega) \tag{7.4}$$

was numerically calculated at different values of τ from the range $0.6 < \tau < 0.95$. At lower τ, we come into the spin-wave region, and $S^{zz}(\mathbf{q},\omega)$ becomes exponentially small due to the factor $\exp(-T_C/T)$ in the low-temperature asymptotics of integral (6.10). On the other hand, when $\tau \to 1$, we get into the critical region where the physics of spin fluctuations is completely different. Analysis shows that $S^{zz}(\mathbf{q},\omega)$ is not changed qualitatively if the parameter υ amounts to several units, therefore, we took $\upsilon = 3$ for the numerical calculations.

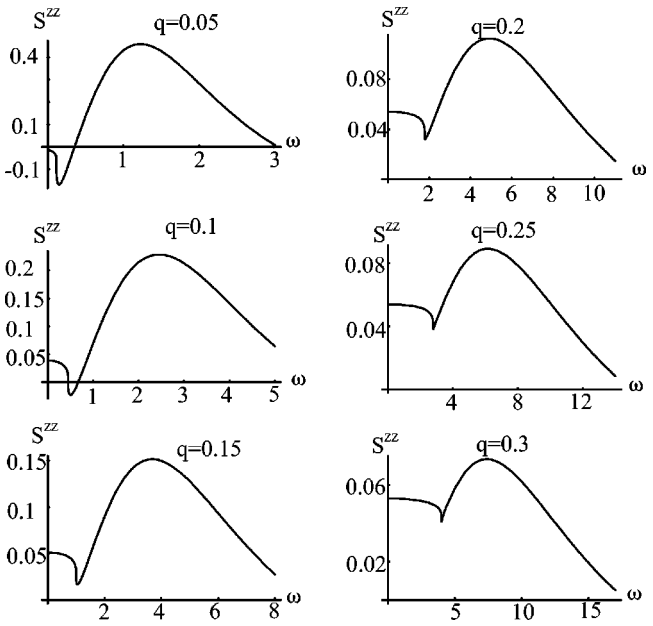

FIG. 13. The longitudinal part of the dynamic structure factor $S^{zz}(\mathbf{q},\omega)$ as a function of dimensionless frequency ω (measured in units 10^{-2}) at $\tau = 0.8$ and different wave vectors q.

In Fig. 13, we plot an example of numerical calculations of the frequency dependence $S^{zz}(\mathbf{q},\omega)$ at various values of the wave vector and fixed temperature. In all the calculations, we accepted the values of parameters $S = 1$ and $z = 6$. We observe a three-peak structure with two wide maxima at frequencies $\pm\omega_q$ and a sufficiently narrow central peak of a lower intensity. With growing q, the height of the central peak approaches the height of the ω_q peak, and they tend to merge and form a broad distribution in the spectrum.

The width of the ω_q peak grows with increasing q. When the temperature changes, the form of the spectral distribution is not changed qualitatively, and only the intensities of peaks and their widths are changed. The behavior of the position of the resonance peak ω_q and its half-width $\Delta\omega_q$ as a function of q at different τ is shown in Fig. 14. A practically linear behavior of ω_q as a function of q is observed that corresponds to the approximate analytic result (7.2). Also, the half-width $\Delta\omega_q$ changes linearly with q, and at a fixed temperature, the ratio $\Delta\omega_q / \omega_q$ is smaller than unity. This allows us to assume that in the system, there do exist wave vibrations of longitudinal components of spins, though with a strong attenuation. At the same time, in the system of longitudinal fluctuations, there is also the relaxation mode connected with the central peak, but, as it is seen from Fig. 13, it strongly interacts with the wave mode at large q.

The intensity of the ω_q peak depends on the temperature and wave vector. It sharply increases when approaches T_C, the stronger, the smaller q (Fig. 15). The tendency of $S^{zz}(\mathbf{q},\omega)$ when $q \to 0$ and $T \to T_C$ to a singular behavior tes-

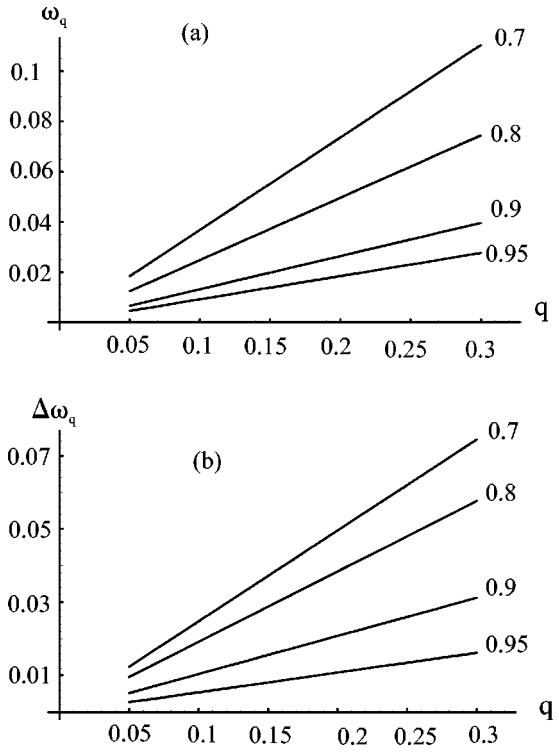

FIG. 14. The q dependences of the position of the $S^{zz}(\mathbf{q},\omega)$ maximum (a) and the half-width $\Delta\omega_q$ (b) for different temperatures τ.

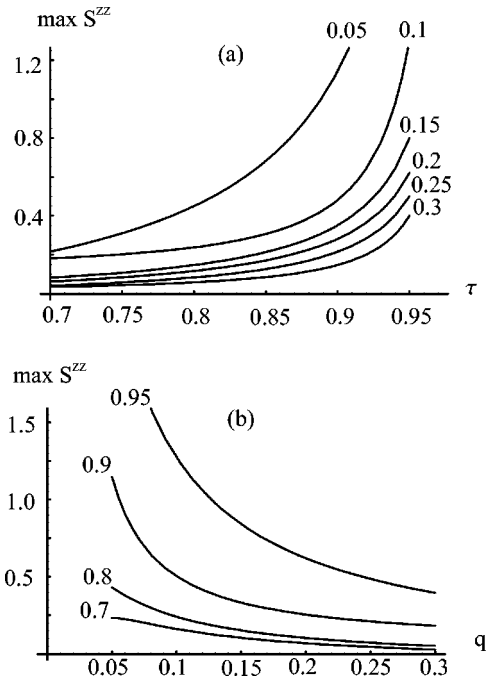

FIG. 15. The dependence of the ω_q-peak intensity in $S^{zz}(\mathbf{q},\omega)$ on temperature τ at different q (a) and on wave vector q for different τ (b).

tifies to the proximity of the hydrodynamic regime. Our GRPA results hold valid beyond the limits of the hydrodynamic regime determined by the condition

$$q \ll \kappa; \quad \kappa = 1/\xi = \sqrt{1-\tau}, \quad (\tau \to 1), \tag{7.5}$$

signifying that the wave vector is far smaller than the inverse correlation length ξ. The physics of fluctuations in the hydrodynamic region is known to be determined[26] by the conservation laws (magnetization); therefore the behavior of fluctuations with large q, we describe within the framework of GRPA, cannot follow from the GRPA. Nevertheless, we see from Fig. 15 that both these regions are sewn together.

Let us note that the spectral distribution (Fig. 13) for small $q=0{,}1$ has a negative region at low frequencies. However, in this case, $\kappa \approx 0.45$. So, it turns out that the condition of hydrodynamic approximation holds valid for this case, therefore any other approximation (in the given case, GRPA) should fail in this region. At lower temperatures, κ grows, therefore the negative regions of the spectrum are set in at larger values of q. It follows from numerical calculations that the negative regions appear in the spectral distribution at $q \approx (3-4)\kappa$. Consequently, at these q and τ, the GRPA fails to work, and fluctuations should be described by the hydrodynamic theory.

Notice also that the dynamic structure factor at large ω beyond the ω_q maximum takes for a moment negative values and then again comes back to positive values. We think that this is an artifact caused by inaccurate calculations of loops $\Pi(q)$, $\Lambda(q)$, $Q(q)$, and $\Phi(q)$ that determine the dynamic susceptibility.

Thus, we conclude that in the region of investigated temperatures $0.6 < \tau < 0.95$, the three-peak structure arises with two neighboring broad peaks that draw together when approaching T_c and form a continuous distribution that can be observed in a neutron experiment as a unique broad peak centered at the zeroth frequency. The distribution width changes linearly with q. Apparently, the contradictory results of neutron studies of longitudinal fluctuations in ferromagnets (when some researchers observe two peaks; whereas the others, one broad maximum) are caused by a particular regime controlled by the temperature and parameters of the model (quantities S,z,v and dispersion relations for the spin-wave spectrum).

VIII. CONCLUSIONS

In the present paper, a diagrammatic technique for spin operators has been newly formulated and used to study the longitudinal spin dynamics in the Heisenberg ferromagnet. Our results describe a region in the $(\mathbf{q},\omega)$ space beyond both the hydrodynamical and the critical regimes for $T < T_C$. The longitudinal spin dynamics that is due to virtual multi-spin-wave processes was studied and discussed in great detail, and the main physics here was captured already within a simple approximation based on a quadratic spin-wave dispersion law. As the central result, we have shown that the dynamic structure factor for longitudinal spin components exhibits generally a three-peak structure including, first, two wide maxima at frequencies $\Omega_q \sim \pm J\langle S^z\rangle q$ corresponding to damped wave modes and, second, a sufficiently narrow and less intensive central peak. When approaching the Curie temperature, the intensity of the latter grows, and all three peaks

form a broad distribution with the linearly q-dependent width. In some experiments this distribution is interpreted as an entire diffusive peak. This observation provides a natural explanation for the seemingly conflicting experimental observations of two-peaked and single-peaked behavior, found in numerous inelastic neutron scattering studies of ferromagnetic materials.

We recall that the critical dynamics of the longitudinal spin components in the isotropic antiferromagnet below the critical temperature $T<T_N$ (T_N is the Néel temperature), has been investigated thoroughly both theoretically[27] and with the inelastic neutron scattering measurements.[12,28] In particular, the dynamic renormalization-group analysis showed that for $\omega\neq 0$, the peaks in the spin spectral density at $T=T_N$ develop smoothly with decreasing temperature, $T<T_N$, into standard spin waves describing transverse spin fluctuations in the hydrodynamic regime. At the same time, it was predicted that the longitudinal spin components behave rather differently, and while crossing over from the hydrodynamical to the critical regime, the coefficient of a spin diffusion becomes divergent. The authors of Ref. 27 supposed that such a behavior for $T<T_N$ could be described by taking into account all the loop diagrams built from transverse spin Green functions. Regarding the ferromagnetic case, in the present paper, we have shown that summation of just this kind of diagrams is of vital importance to properly describe the longitudinal spin dynamics.

Study of the longitudinal spin dynamics in the isotropic Heisenberg antiferromagnet is in progress. At the present stage, our investigation confirms the multi-spin-wave nature of longitudinal spin dynamics in the ferromagnet suggested in the early studies of the quantum[4] and the classical[13] Heisenberg models for $T<T_C$. It should be emphasized once more that the present analysis involves strongly renormalized spin-wave excitations existing at high temperature, rather than the linear spin waves describing a transverse spin component motion near the magnetic ground state.

ACKNOWLEDGMENTS

The authors (Yu. I. and V. Yu.) are grateful to Professor P. Fulde for hospitality during their stay at MPI PKS where this work was finished. We thank Nic Shannon for critical reading of the manuscript and useful remarks. This work was supported in part by the Russian Foundation for Basic Research, project 00-15-95544.

APPENDIX

Consider a thermal average of a T-ordered operator product $A(\tau_1)$, $B(\tau_2)$, $C(\tau_3)$, ..., where τ_1, τ_2, τ_3, ... are thermodynamic "times:"

$$((TA(\tau_1)B(\tau_2)C(\tau_3)\ldots e^V)) \equiv \mathrm{Tr}[e^{-\beta H}TA(\tau_1)B(\tau_2)C(\tau_3)\cdots e^V],$$

Here H is the Hamiltonian and the operator V describes interactions of the system under consideration with fluctuating external fields. Differentiation with respect to τ_1 yields

$$\begin{aligned}\frac{\partial}{\partial\tau_1}((TA(\tau_1)B(\tau_2)C(\tau_3)\cdots e^V)) &= ((T\dot{A}(\tau_1)B(\tau_2)C(\tau_3)\cdots e^V))+((T\{A(\tau_1),B(\tau_2)\}\\ &\times C(\tau_3)\cdots e^V))+((T\{A(\tau_1),C(\tau_3)\}B(\tau_2)\cdots e^V))\\ &+\cdots+((T\{A(\tau_1),V\}B(\tau_2)C(\tau_3)\cdots e^V)).\end{aligned} \tag{A1}$$

Here $\dot{A}$ is given by

$$\dot{A}=\frac{\partial A}{\partial\tau}=-[A,H]_-, \quad A(\tau)=e^{\tau H}Ae^{-\tau H},$$

and the notation $\{\ldots,\ldots\}$ denotes

$$\{A(\tau),X(\tau')\}\equiv\delta(\tau-\tau')[A,X]_-. \tag{A2}$$

for commuting operators or

$$\{A(\tau),X(\tau')\}\equiv\pm\delta(\tau-\tau')[A,X]_+, \tag{A3}$$

for anticommuting ones. The sign in Eq. (A3) is determined, as usual, by a parity of the number of that permutations within the sequence $(ABC\ldots X\ldots)$ one needs to remove the operator X to the first position.

The identity (A1) can be proved by expanding the exponential function e^V in a power series and applying, at the final stage, the inverse operation. This identity should be regarded as the equation of motion for the Green functions of the system in fluctuational fields.

[1] S. V. Tayablikov, *Methods in the Quantum Theory of Magnetism* (Plenum, New York, 1967).
[2] F. Dyson, Phys. Rev. **102**, 1217 (1956).
[3] N. N. Bogoliubov and S. V. Tyablikov, Dokl. Akad. Nauk SSSR **126**, 53 (1959) [Sov. Phys. Dokl. **4**, 589 (1960)].
[4] V. G. Vaks, A. I. Larkin, and S. A. Pikin, Zh. Eksp. Teor. Phys. **53**, 1089 (1967) [Sov. Phys. JETP **26**, 647 (1968)].
[5] O. W. Dietrich, J. Als-Nielsen, and L. Passell, Phys. Rev. B **14**, 4923 (1976).
[6] P. W. Mitchell, R. A. Cowley, and R. Pynn, J. Phys. C **17**, L875 (1984).
[7] J. Villan, in *Critical Phenomena in Alloys, Magnets and Superconductors*, edited by A. J. Millis (McGraw-Hill, New York, 1971), p. 423.
[8] G. F. Mazenko, Phys. Rev. B **14**, 3933 (1976).
[9] M. F. Collins, V. J. Minkiewicz, R. Nathans, L. Passel, and G. Shirane, Phys. Rev. **179**, 417 (1969).
[10] V. J. Minkiewicz, M. F. Collins, R. Nathans, and G. Shirane, Phys. Rev. **181**, 920 (1969).
[11] J. Als-Nielsen, O. W. Dietrich, and L. Passel, Phys. Rev. B **14**, 4908 (1976).
[12] U. J. Cox, R. A. Cowley, S. Bates, and L. D. Cussen, J. Phys.: Condens. Matter **1**, 3031 (1989).
[13] A. Bunker and D. P. Landau, Phys. Rev. Lett. **85**, 2601 (2000).

[14] Yu. A. Izyumov and F. A. Kassan-Ogly, Fiz. Met. Metalloved. **26**, 385 (1968); **30**, 225 (1970).
[15] Yu. A. Izyumov, F. A. Kassan-Ogly, and Yu. N. Scryabin, *Field Methods in Theory of Ferromagnetism* (Fiziko-Matematicheskaya Literatura, Moscow, 1974), in Russian.
[16] Yu .A. Izyumov and Yu. N. Scryabin, *Statistical Mechanics of Magnetically Ordered Systems* (Consultants Bureau of Plenum Publ. Corporation, New York, 1988).
[17] G. Baym and L. P. Kadanoff, Phys. Rev. **124**, 287 (1961).
[18] Yu. A. Izyumov and B. M. Letfulov, J. Phys.: Condens. Matter **2**, 8905 (1990).
[19] Yu. A. Izyumov, M. I. Katsnelson, and Yu. N. Scryabin, *Magnetism of Itinerant Electrons* (Fiziko-Matematicheskaya Literatura, Moscow, 1994), in Russian.
[20] R. Silberglitt and A. B. Harris, Phys. Rev. **174**, 640 (1968).
[21] A. B. Harris, D. Kumar, B. I. Halperin, and P. C. Hohenberg, Phys. Rev. B **3**, 961 (1971).
[22] Yu. A. Izyumov and N. I. Chaschin, Fiz. Met. Metalloved. **92**, 451 (2001); **92**, 531 (2001).
[23] R. N. Wilcox, Phys. Rev. **174**, 624 (1968).
[24] P. C. Kwok and T. D. Schultz, J. Phys. C **2**, 1196 (1969).
[25] R. Pirc and B. G. Dick, Phys. Rev. B **9**, 2701 (1974).
[26] D. Forster, *Hydrodynamic Fluctuations, Broken Symmetry and Correlation Functions* (W.A. Benjamin, Massachusetts, 1975).
[27] G. F. Mazenko, M. J. Nolan, and R. Freedman, Phys. Rev. B **18**, 2281 (1978).
[28] R. Coldea, R. A. Cowley, T. G. Perring, D. F. McMorrow, and B. Roessli, Phys. Rev. B **57**, 5281 (1998).